Proceedings of the Second International Conference on Press-in Engineering 2021, Kochi, Japan – Matsumoto et al (eds)

Anticorrosive effect by inserting sheet piles on the sides of underground tunnel at shallow depth

M. Oka, H. Takeda, Z. Wang & K. Maekawa
Yokohama National University, Yokohama, Kanagawa, Japan

ABSTRACT: In recent years, deterioration due to salt damage in underground transmission tunnels which locate near coastal areas has been reported. In the case of the open-cut construction, earth-retaining walls are adopted at the time of excavating workspace. It is expected that the earth-retaining wall may protect underground transmission structures from the stray current. In this study, the macro-cell corrosion of the underground structures is investigated and the possibility of anti-corrosive effect by inserting sheet piles or utilizing existing steel plates is experimentally evaluated. Specimens were prepared by using the mixture made from starch and water to represent soil and steel plates to stand for structures with sheet piles. A simple systematic corrosion experiment was performed. The external charge was applied and ion profiles are measured, and corrosive states were observed. By electrically jacking sheet piles, the suppressing polarization effect with sheet piles against corrosion was found from the experiment.

1 INTRODUCTION

1.1 *Background*

The urban tunnels for the underground transmission system to contain cables usually have two types: excavation tunnels and shield ones. The former ones are constructed by producing open spaces with steel sheet piling and constructing the RC ducts thereafter in the workspace followed by backfill. They are electricity facilities of importance to ensure the stable energy supply in urban areas (see **Figure 1**). They were mostly developed for stable power supply during the period of high economic growth in 1960s. Some of the underground tunnels which have passed over 40 years have corrosive deterioration (Enya *et al.* 2011a, b, Liu *et al*. 2018). The deterioration caused by seawater intrusion has been reported for the underground shield tunnels near seashores (see **Figure 2**).

The groundwater including the detrimental ions flows in the tunnels through segment joints, and it remains at the lower part of the underground tunnel, and steel devices and reinforcement corrode accordingly (Aoki *et al*. 2019). For the open-cut construction, sheet piles are driven in the foundation and earth-retaining walls are established during excavation of the workspace (see **Figure 3**). It is expected that these sheet piles may protect the tunnel structures suffering from the toxic substance and corrosion due to the stray current or large-scale electric circuit. Speaking of anti-corrosion methods of reinforced concrete, as commonly used methods, the cathodic protection in use of sacrificial anodic materials and desalination are being applied (Allen & Larry 2001, Cao 2008).

They are somehow local scale means focusing on the anodic and cathodic polarization whose distance is not large (Hsu *et al*. 2000). In reality, considering the gaps of natural potentials (different metals, ion concentrations, etc.) or external electric charge such as the stray current, the macro-cell corrosion of larger sizes took place (Otsuki *et al*. 2007, Chen *et al*. 2017). For underground reinforced concrete, multi-ions' interaction may exist in the pore solution such as Na^{+}, K^{+}, Mg^{2+}, SO_4^{2-}, seawater (Cl^{-}) and cement hydrates of Ca^{2+}, Al^{3+}, OH^{-}, Si^{2+}. As these ions have much to do with concrete solid, it is required to consider the multi-ion kinetics when we intend to actively control the electric potential which affects structural reinforced concrete (Bazant 1979a, b). This issue has been the engineering problem when railroad tracks are operated with electrical energy (Chen *et al*. 2017, Wang *et al*. 2017).

The objective of this study is to verify the macro-cell corrosion of underground facilities and to discuss the feasibility of using steel sheet piles as an anti-corrosion method. Experiments with specimens made of pseudo-concrete materials were reported (Maekawa *et al*. 2019, 2020, Aoki *et al*. 2020). Here, we may see the locations of polarized anodic-

DOI: 10.1201/9781003215226-41

Figure 1. Interior of utility duct by shield tunneling.

Figure 2. Example of corrosion by salt damage.

cathodic reactions which accompany corrosion products and hydrogen gas. The authors focus on the ionic concentration, since the rising ionic concentration caused by electric protection may deteriorate concrete solid such as ASR (Takahashi *et al*. 2016). Through different cases, we aim to propose an effective anti-corrosion method with steel sheet piles.

1.2 *Scheme of development*

A general flow of the research plan is summarized in **Figure 4** to reach a goal of assessing the macro-cell corrosion with integrating the electric field and ionic

Figure 3. Support system during excavation.

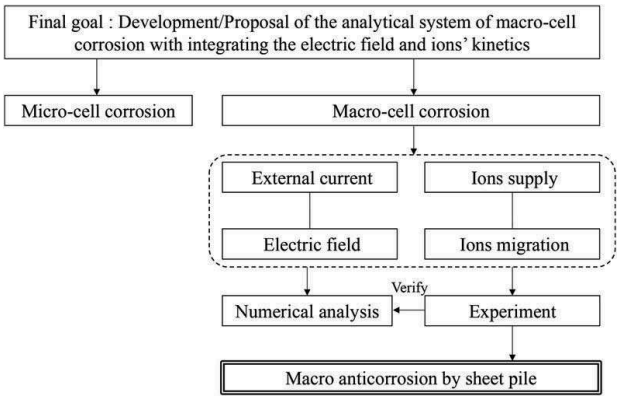

Figure 4. Examination flow.

kinetics. A macro-cell circuit generally brings about severe corrosion which may deteriorate serviceability and ultimate states of underground structural concrete. Electric potential gaps among soil, structure and adjacent facilities will be a source of a large-scale circuit which produces anodic and cathodic polarization. In addition, various ions exist in the soil. Seawater ingredients are included in groundwater near the shore (Otsuki *et al*. 2007). When plural ions exist, the ionic equilibrium may produce self-non-uniform potentials. As the multi-ion kinetics are affected by the electrical field as well and also have an impact on the electrical circuit, which is the coupled effect of electrical field and chemical ion field (Elakneswaran & Ishida 2014).

The electric field and the ion are closely connected to be described by the Nernst-Planck theorem (Na & Xi 2019). Then, the numerical scheme to consider the relation of the electric potential field and the ion concentration gradient is required. In this study, the experiment was carried out to verify the macro-cell corrosion system in association with ion profiles and the locations of anodic-cathodic polarization. The experimental facts serve to examine the qualitative understanding for sheet pile usages as

a protection against corrosion of underground facilities and will take part in validation of the numerical analysis.

2 CORROSION EXPERIMENT

2.1 *Specimens preparation*

Pseudo-concrete materials were used instead of concrete and soil in order to measure the ion concentration easily. The pseudo-concrete materials in the current study were starch mixture, which was different from the past research where transparent polymer was adopted (Maekawa *et al*. 2019, 2020, Aoki 2020). The mix proportion of the specimen is listed in **Table 1**.

NaCl and $Ca(OH)_2$ were mixed with water and starch. The mixture was poured into a plastic container with dimension of 220x150x45 mm^3 and the height of specimen was 15 mm. Steel plates were utilized as electrodes which were inserted vertically between the starch and inner walls of the container on left and right sides. One iron plate was placed in the middle to represent the underground tunnel.

Five specimens were prepared in the current experiment, as shown in **Figure 6**: ① Case 1 was the referenced specimen where the middle steel plate was placed parallelly to the external charge direction; ② Case 2 had two vertical steel plates (to simulate the sheet piles) inserted perpendicular to the charge direction on both right and left sides; ③ Case 3 had a similar arrangement as Case 2 but the difference was that the sheet piles were connected with metal wires;

Table 1. Mix proportion of the specimens.

starch (g)	H_2O (ml)	NaCl (g)	$Ca(OH)_2$ (g)
270	270	5	5

Figure 5. Schematic of non-countermeasure (Case 1).

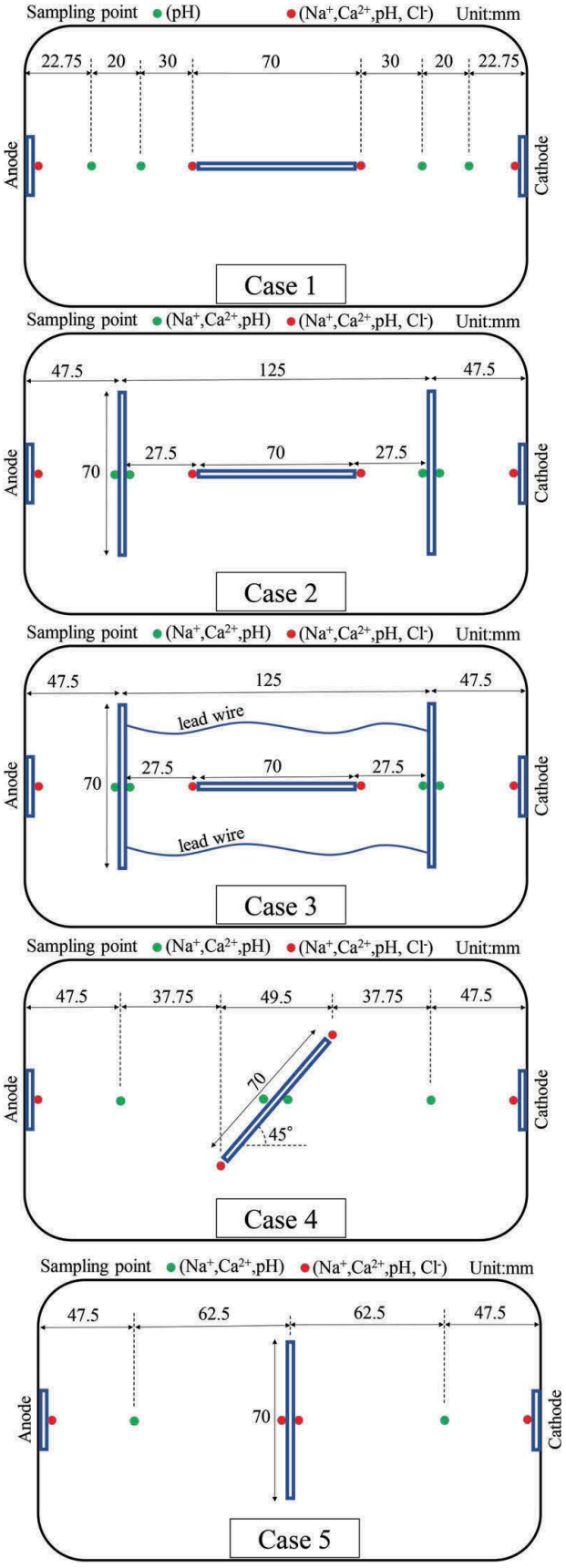

Figure 6. Sampling points.

④, ⑤: Case 4 and 5 had similar arrangements with Case 1 but the iron plates had different angles with the external charge direction (45° and 90°). It should be noted that Case 1, the referenced case was simulating the underground tunnels without any protection as shown in **Figure 6**. Case 1, 2 and 3 were performed to confirm the anti-corrosion effect when adopting sheet piles on the sides of the underground tunnel. Case 4 and 5 were adopted to investigate the macro-cell corrosion distribution with different directions of the stray current.

2.2 *Electrical charge and ion measurement*

The external charge of 6V was applied to the electrode with 4 hours for Case 1, 2 and 3 while 40 hours for Case 4 and 5. The pH and several ions' concentrations were measured at 0h, 2h and 4h after charging. The pH value was measured with a pH sensor. And the chloride testing tubes were used for measurement of chloride ions while the electronic sensors were utilized to measure the sodium and calcium concentrations. The measurement points are shown in **Figure 6** where the green points mean the measured positions of Na^+, Ca^{2+} and pH. The red points mean the measured positions of Na^+, Ca^{2+}, pH and Cl^-. The measurement points of Cl^- become less than other items because the number of Cl^- testing tubes was limited. Samples were taken out and diluted by 100 times to match the limit requirement of the measurement range of measuring sensors for sodium and calcium ions.

3 RESULTS AND DISCUSSIONS

3.1 *Visual evaluation of corrosion*

The results of macro-cell corrosion were given in **Figure 7**. An obvious polarization was captured where the anodic regions showed oxidation of iron and production of rust while air bubbles (hydrogen) were released at the cathodic regions. Compared with the corrosion products of Case 1, it turned out that the quantity of rust at anode was much less in Case 2 or 3 by naked-eye observation. As a result, it indicated that the underground tunnel (horizontal steel plate) was protected by the sheet piles (vertical steel plates). In this paper, quantitive observation was the focus thus the precise corrosion amount was not measured.

Furthermore, the anti-corrosion effect was more effective if connecting the sheet piles with metal wires (Case 3). Case 4 and 5 showed the symmetric properties of the anodic and cathodic polarization.

3.2 *Ion concentration profiles*

The description of concentration change with time are shown together with the corrosion conditions in

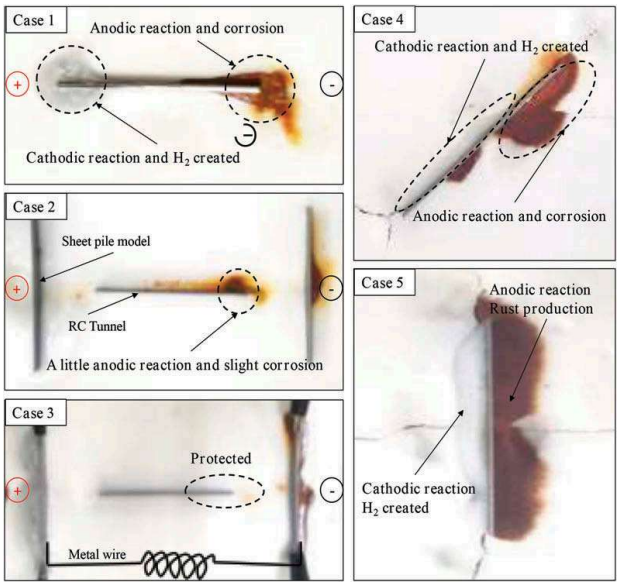

Figure 7. Summaries of the corrosion conditions.

Figure 8. The measured ion concentrations are shown in **Figure 9-12**. The samples were diluted 100 times with water.

In Case 1, the ion concentration changes were found in both anodic and cathodic regions, which could be explained by the polarization reactions:

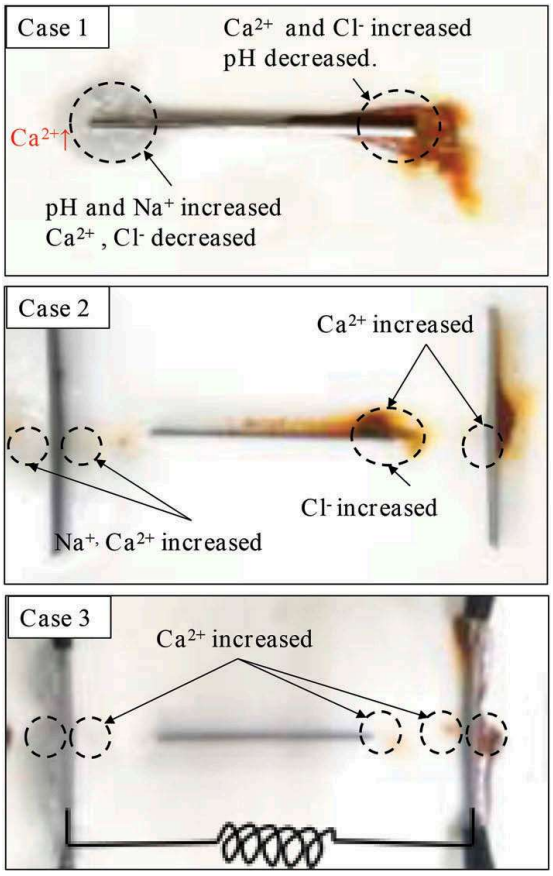

Figure 8. Description of the measured ion concentration.

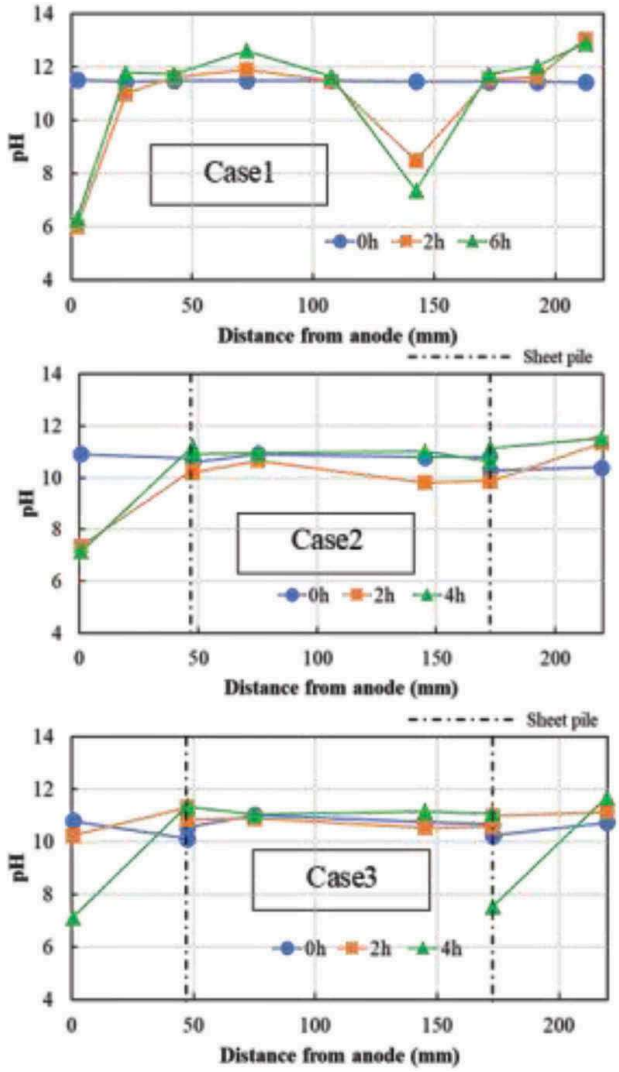

Figure 9. Measured value of pH.

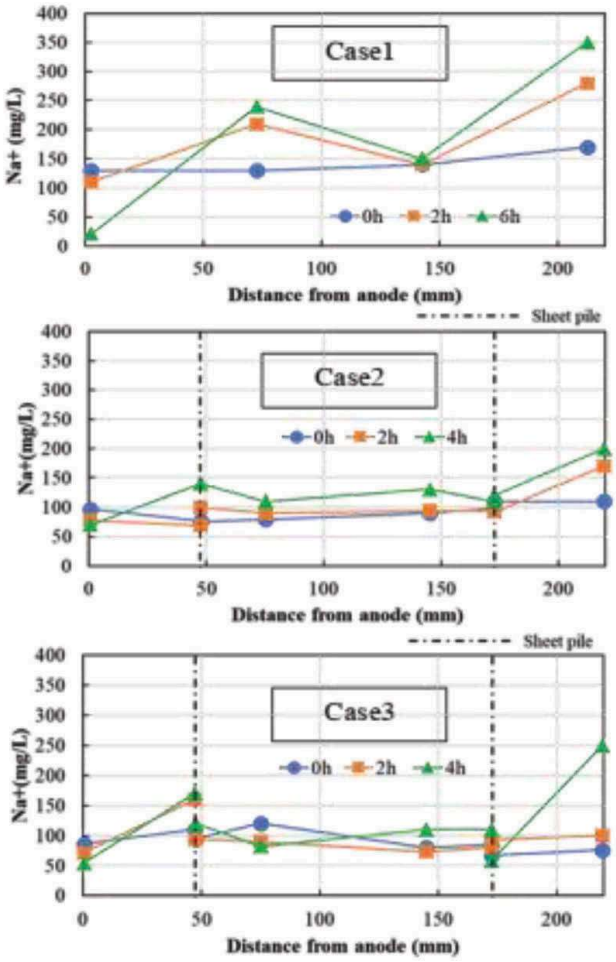

Figure 10. Measured value of sodium ion concentration.

hydroxide ions were consumed in anode and created in cathode; Cation Na^+ gathered towards cathode while moved away from anode; Oppositely, Cl^- increased near anode while decreased near cathode. These phenomena could be well explained so far. However, the notable point was Ca^{2+} concentration in the experiment. It was found that Ca^{2+} showed an opposite result which increased near the anodic electrode. The reason was explained in **Figure 13**: as anion, OH^- ion moved towards the anodic electrode and resulted in the increased ion concentration, see the black curve in **Figure 13**. Then the OH^- ion near anode would with Fe^{2+} ion, which was generated from the combine oxidation of the anode material – steel. Then OH^- ion would decrease near the anode as the red curve in **Figure 13**. At the same time, cations Ca^{2+} moved away from anode and met the coming OH^- ions and combined into $Ca(OH)_2$ and precipitated into white crystal. As a result, some Ca^{2+} ions were trapped near the anode, which lead to an increasing amount of Ca^{2+} concentration. This phenomenon was also captured by the previous experiment by Maekawa *et al*. (2020), as **Figure 14**.

4 PROPOSAL OF ANTI-CORROSION SYSTEM

From the experiment, the proposal of the anti-corrosion system is the modification of Case 3. In a practical application, it is suggested to apply the electrical charge to the sheet piles as illustrated in **Figure 15**. For example, as corrosion takes place on the left-bottom of the underground facilities because of stagnant salty water, it is possible to apply anodic electrode on the corroded side (left), while the cathodic electrode on the opposite (right). From the knowledge obtained from the experiment, the corrosion part will be protected (cathodic reaction) while a new corrosion would happen on the top-right because of inevitable polarization.

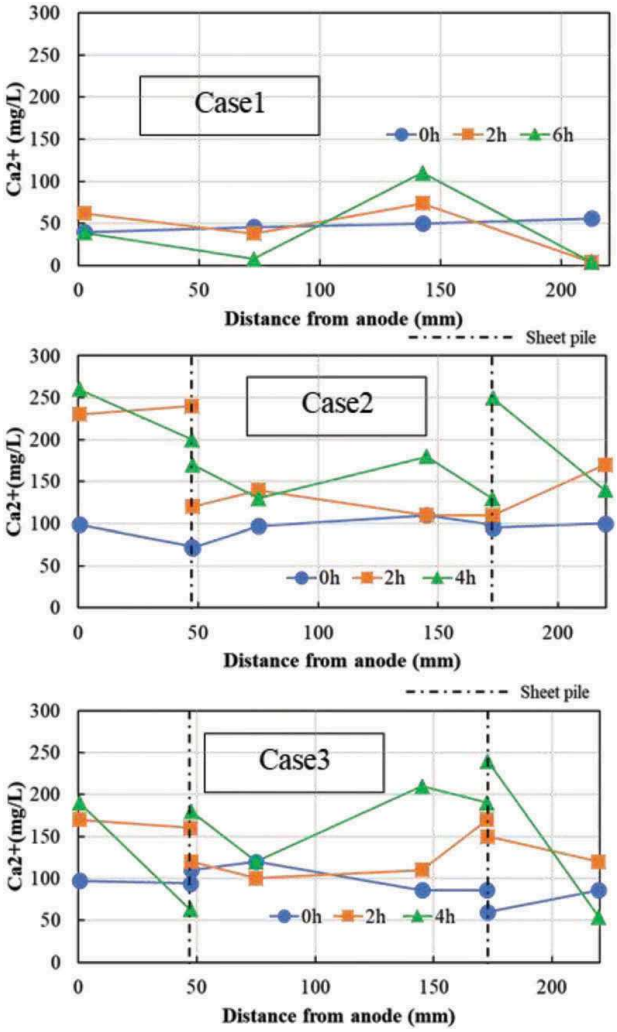

Figure 11. Measured value of calcium ion concentration.

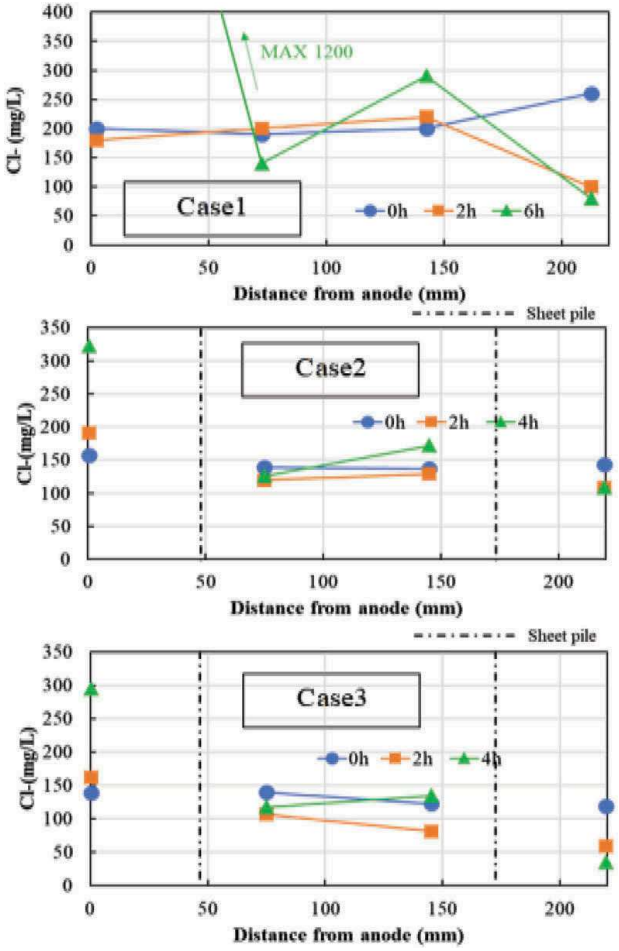

Figure 12. Measured value of chloride ion concentration.

However, it would be acceptable if the corrosion part would be transferred from the mechanically-risky place to non-problematic places (Fan *et al.* 2020). Thus, through this systematic macro-cell analytical method, the corrosion could be controlled not locally but with consideration of the wider domain (underground structures, sheet piles and soil foundation). Although voltage is not directly applied to the sheet pile in Case 3, but it indicates that the underground tunnel is protected. Meanwhile, the protected place would have increased concentration of cation such as K^+ or Na^+ as well as the alkalinity, which may lead to problems of alkali-silica reaction for the concrete. Thus, it is of great significance to have an overall understanding of the coupled chemical and electrical fields as well as the mechanical issue so as to propose the optimized anti-corrosion method.

In current study, the sheet piles are adopted as the anti-corrosion protector. It should be noted that the cost might be quite different in terms of whether the sheet piles are already existing in the ground, or they need additional execution of inserting. Especially, this paper would like to discuss the possibility of using existing sheet piles, which are left in soil after construction to prevent the consolidation of adjacent

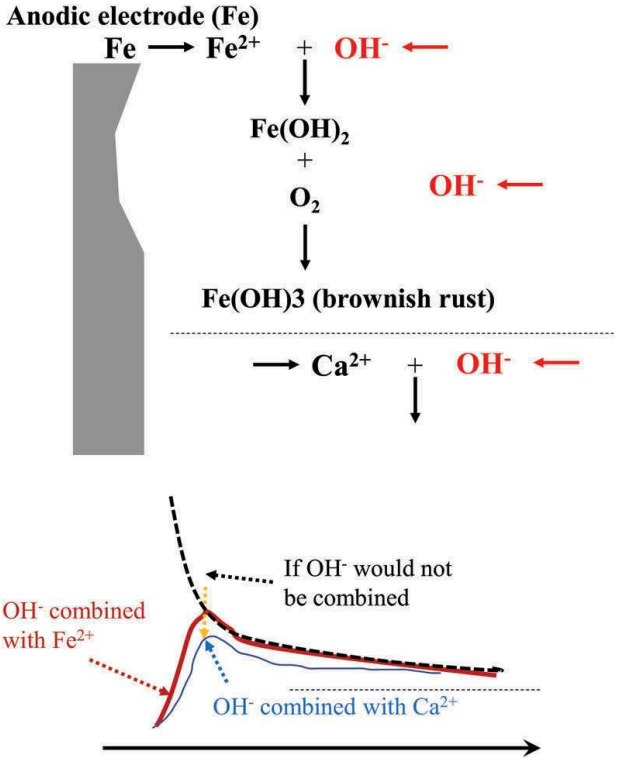

Figure 13. Mechanism explanation with $Ca(OH)_2$ precipitation.

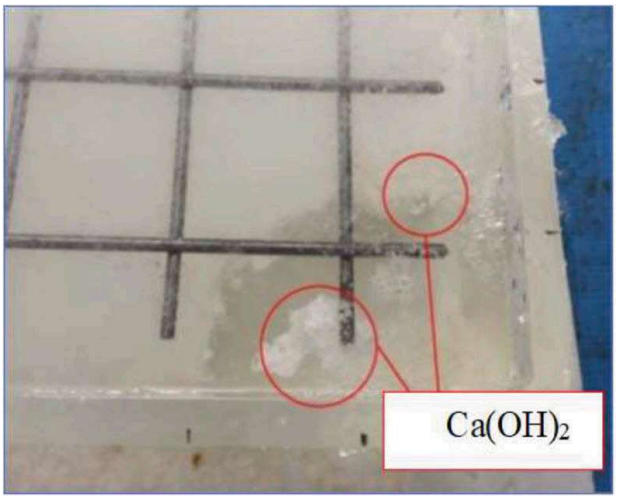

Figure 14. Observation of $Ca(OH)_2$ precipitation (Maekawa *et al*. 2020).

foundation (JASPP, 2017). Then the cost is mainly coming from the impressed charge, which might be low to trigger the reverse macro-cell current depending on the present circuit. As an important factor, soil saturated with underground water is required to assure the diffusivity of ions and thus the conductivity of ground as the electrolyte.

5 CONCLUSIONS

(1) The experiment was conducted with starch specimens and steel plates under external charge to simulate the underground systems including tunnels, sheet piles and soil foundation. The polarization locations and change of ion concentrations were observed, which obeyed the electrochemical theory.
(2) Besides the common sense where anions gather near anode and cations gather near cathode, the tendency of increasing Ca^{2+} near the anode was observed, which was explained with the ion flux and zero current theories under the coupled electrical and chemical fields.
(3) To apply external charge to the already existing or newly inserted sheet piles was proposed as the anti-corrosion method. But careful attention should be paid on the multi-ion profiles in the whole system with respect to the alkali-silica reaction. And the mechanical behavior of the underground structures should also be clarified along with the anti-corrosion application.

ACKNOWLEDGEMENT

The authors would like to express their sincere gratitude to the financial support by the Grant-in-Aid for JSPS Fellows (No. P20367).

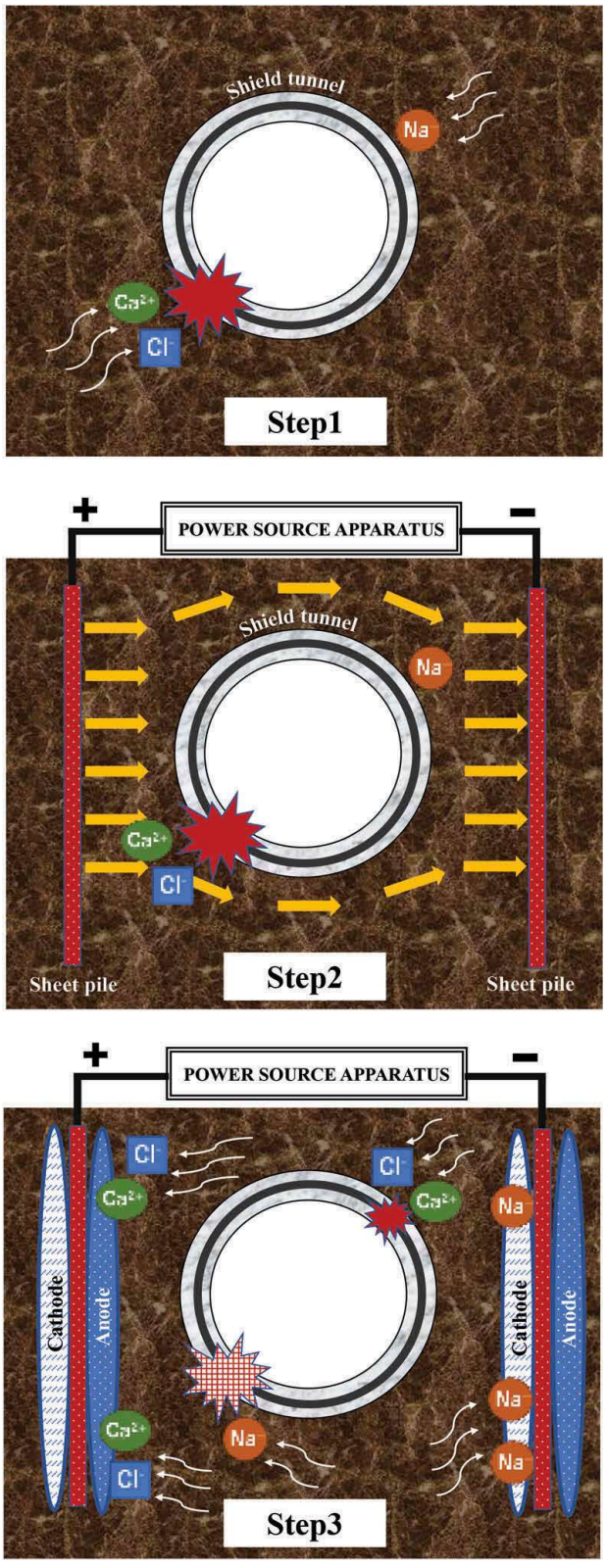

Figure 15. Illustration of the anti-corrosion system.

REFERENCES

Allen, J. B. & Larry, R. F. 2001. *Electrochemical methods fundamentals and applications*. New York: John Wiley & Sons.
Aoki, H., Takahashi, H. & Maekawa, K. 2019. Evaluation study of polarization reaction region by electric

corrosion experiment of reinforcing steel using visualization materials. *Proceedings of Japan Concrete Institute* 42 (1): 761–766.

Bazant, Z. P. 1979a. Physical model for steel corrosion in concrete sea structures – theory. *Journal of the Structural Division* 105 (6): 1137–1153.

Bazant, Z. P. 1979b. Physical model for steel corrosion in concrete sea structures – application. *Journal of the Structural Division* 105 (6): 1155–1166.

Cao, C. 2008. *Principles of electrochemistry of corrosion*. Beijing: Chemical Industry Press.

Chen, Z., Koleva, D. & van Breugel, K. 2017. A review on stray current-induced steel corrosion in infrastructure. *Corrosion Reviews* 35(6): 397–423.

Elakneswaran, Y. & Ishida, T. 2014. Development and verification of an integrated physicochemical and geochemical modelling framework for performance assessment of cement-based materials. *Journal of Advanced Concrete Technology* 12 (4): 111–126.

Enya, Y., Anan, K., Otsuka, M. & Koizumi, A. 2011a. Study on maintenance of the tunnel for the underground transmission. *Proceedings of Japan Concrete Institute* 67(2): 108–125.

Enya, Y., Naito, Y., Anan, K., Otsuka, M. & Koizumi, A. 2011b. Study of reinforcement design for deteriorated shield tunnel. *Journal of Japan Society of Civil Engineers, Ser. F1 (Tunnel Engineering)* 67 (2): 62–78.

Fan, S., Cui, Y. & Maekawa, K. 2020. Failure mode of deteriorated underground RC structures with hollow circular cross-section. *Proceedings of 2020 International Conference on Civil, Architectural and Environmental Engineering, Christchurch, 23-25 November 2020*.

Hsu, K. L., Takeda, H. & Maruya, T. 2000. Numerical simulation on corrosion of steel in concrete structures under chloride attack. *Doboku Gakkai Ronbunshu* 2000 (655): 143–157.

Japan Association for Steel Pipe Piles. 2017. *Kouyaita Q&A (Steel Sheet Piles Q&A). Kawasaki: Hokushin. (in Japanese)*

Liu, S. He, C., Feng, K. & An. Z. 2018. Research on corrosion deterioration and failure process of shield tunnel segments under loads. *China Civil Engineering Journal* 51 (6): 120–128.

Maekawa, K., Okano, Y. & Gong, F. 2019. Space-averaged non-local analysis of electric potential for polarization reactions of reinforcing bars in electrolytes, *Journal of Advanced Concrete Technology* 17(11): 616–627.

Maekawa, K., Takeda, H. & Wang, Z. 2020. Multi-ion equilibrium and migration model in pore solution of sea water concrete. *Proceedings of the Third International Workshop on Seawater Sea-sand Concrete (SSC) Structures Reinforced with FRP Composites, Shenzhen, 11-12 January 2020*.

Na, O. & Xi, Y. 2019. Parallel finite element model for multispecies transport in nonsaturated concrete structures. *Materials* 12(17): 2764.

Otsuki, N., Min, A. K., Madlangbayan, M. & Nishida, T. 2007. A study on corrosion of paint-coated steel with defects in marine environment. *Doboku Gakkai Ronbunshuu* 63 (4): 667–676.

Takahashi, Y., Ogawa, S., Tanaka, Y. & Maekawa, K. 2016. Scale-dependent ASR expansion of concrete and its prediction coupled with silica gel generation and migration. *Journal of Advanced Concrete Technology* 14 (8): 444–463.

Wang, C., Li, W., Wang, Y., Xu, S. & Fan, M. 2018. Stray current distributing model in the subway system: A review and outlook. *International Journal of Electrochemical Science*. 13(2): 1700–1727.